

Towards the discovery of new physics with lepton-universality ratios of $b \rightarrow s\ell\ell$ decays

Li-Sheng Geng¹, Benjamín Grinstein², Sebastian Jäger³, Jorge Martin Camalich⁴, Xiu-Lei Ren^{5,6} and Rui-Xiang Shi¹

¹*School of Physics and Nuclear Energy Engineering and International Research Center for Nuclei and Particles in the Cosmos, Beihang University, Beijing 100191, China*

²*Dept. Physics, University of California, San Diego, 9500 Gilman Drive, La Jolla, CA 92093-0319, USA*

³*University of Sussex, Department of Physics and Astronomy, Falmer, Brighton BN1 9QH, UK*

⁴*CERN, Theoretical Physics Department, CH-1211 Geneva 23, Switzerland*

⁵*State Key Laboratory of Nuclear Physics and Technology, School of Physics, Peking University, Beijing 100871, China*

⁶*Institut für Theoretische Physik II, Ruhr-Universität Bochum, D-44780 Bochum, Germany*

Tests of lepton-universality as rate ratios in $b \rightarrow s\ell\ell$ transitions can be predicted very accurately in the Standard Model. The deficits with respect to expectations reported by the LHCb experiment in muon-to-electron ratios of the $B \rightarrow K^{(*)}\ell\ell$ decay rates thus point to genuine manifestations of lepton non-universal new physics. In this paper, we analyse these measurements in the context of effective field theory. First, we discuss the interplay of the different operators in R_K and R_{K^*} and provide predictions for R_{K^*} in the Standard Model and in new-physics scenarios that can explain R_K . We also provide approximate numerical formulas for these observables in bins of interest as functions of the relevant Wilson coefficients. Secondly, we perform frequentist fits to R_K and R_{K^*} . The SM disagrees with these measurements at 3.7σ significance. We find excellent fits in scenarios with combinations of $\mathcal{O}_{9(10)}^\ell = \bar{s}\gamma^\mu b_L \ell\gamma_\mu(\gamma_5)\ell$ operators, with pulls relative to the Standard Model in the region of 4σ . An important conclusion of our analysis is that a lepton-specific contribution to \mathcal{O}_{10} is important to understand the data. Under the hypothesis that new-physics couples selectively to the muons, we also present fits to other $b \rightarrow s\mu\mu$ data with a conservative error assessment, and comment on more general scenarios. Finally, we discuss new lepton universality ratios that, if new physics is the origin of the observed discrepancy, should contribute to the statistically significant discovery of new physics in the near future.

I. INTRODUCTION

Ratios of decay rates such as $B \rightarrow K^{(*)}\ell\ell$ for different leptons $\ell = e$ or μ are protected from hadronic uncertainties and can be very accurately predicted in the Standard Model (SM) [1, 2]. Therefore, significant discrepancies with experiment in these observables would have to be interpreted as unambiguous signals of new physics (NP) that, in addition, must be related to new lepton non-universal interactions. After first measurements reporting no significant deviation from universality (within large experimental uncertainties) at B -factories [3–5], in 2014 the LHCb collaboration reported a quite precise measurement of the ratio $R_K = \Gamma(B \rightarrow K\mu\mu)/\Gamma(B \rightarrow Kee)$ [6]

$$R_K = 0.745_{-0.074}^{+0.090} \pm 0.036, \quad (1)$$

in the bin corresponding to dilepton mass squared $q^2 \in [1, 6] \text{ GeV}^2$ that deviated from the SM predictions $R_K = 1.0004(8)$ [1, 2] with a significance of 2.6σ . Recently, the LHCb reported the measurement of $R_{K^*} = \Gamma(B \rightarrow K^*\mu\mu)/\Gamma(B \rightarrow K^*ee)$ in two bins of q^2 [7],

$$R_{K^*}[0.045, 1.1] \text{ GeV}^2 = 0.660_{-0.070}^{+0.110} \pm 0.024, \quad R_{K^*}[1.1, 6] \text{ GeV}^2 = 0.685_{-0.069}^{+0.113} \pm 0.047, \quad (2)$$

where the first error is statistical the second systematic, and which show again deficits with respect to the SM predictions (see below),

$$R_{K^*}^{\text{SM}}[0.045, 1.1] \text{ GeV}^2 = 0.920(7), \quad R_{K^*}^{\text{SM}}[1.1, 6] \text{ GeV}^2 = 0.996(2), \quad (3)$$

with a significance of 2.3σ and 2.4σ , respectively.

In addition, during the last few years there have been considerable investigations related to tensions with SM predictions in the angular analysis of $B \rightarrow K^*\mu\mu$ [8–12] and in branching fractions [13–15] whose significance have been claimed to be in the $4 - 5\sigma$ range in some global analyses [16–18], although these observables are afflicted by hadronic uncertainties that obscure the interpretation and significance of the anomaly [19–36]. On the other hand, if the NP coupled selectively to the muons, then the effect that would be needed to explain the R_K anomaly could also naturally explain these other anomalies in the angular distributions and rates [37–40]. Several authors have proposed combinations of the angular observables of $B \rightarrow K^{(*)}\ell\ell$ for muons and electrons probing lepton universality, that are again protected from hadronic uncertainties and sensitive to specific scenarios of NP [29, 41–43]. Indeed, some of these observables have been recently analysed by the Belle [10] collaboration showing overall consistency with the SM, albeit with large experimental errors.

In this paper, we perform an analysis of the R_{K^*} measurements together with R_K and other $b \rightarrow s\mu\mu$ data. First, we describe the dependence of the relevant lepton-universality ratios on lepton-specific Wilson coefficients of the weak Hamiltonian of

$b \rightarrow s\ell\ell$ transitions, focusing in the correlations induced between R_K and R_{K^*} . We then present numerical predictions for R_K and R_{K^*} in the SM and in benchmarks scenarios of NP for the bins of interest and present numerical formulas for their dependence on the Wilson coefficients. Finally, we present a series of fits to the data, including in subsequent steps the $B_s \rightarrow \mu\mu$ branching fraction and all the measurements of CP -averaged combinations of angular observables of $B \rightarrow K^*\mu\mu$ at low q^2 . We describe our findings in terms of frequentist statistic inference and discuss the robustness of the results to variations of hadronic uncertainties.

II. STRUCTURE OF THE NEW-PHYSICS CONTRIBUTIONS TO $R_{K^{(*)}}$

To leading order in G_F the effective Hamiltonian for $b \rightarrow s\ell\ell$ transitions at low-energies ($\mu \sim m_b$) in the SM is [44–46]

$$\mathcal{H}_{\text{eff}}^{\text{SM}} = \frac{4G_F}{\sqrt{2}} \sum_{p=u,c} \lambda_{ps} \left(C_1 \mathcal{O}_1^p + C_2 \mathcal{O}_2^p + \sum_{i=3}^{10} C_i \mathcal{O}_i \right), \quad (4)$$

with $\lambda_{ps} = V_{pb}V_{ps}^*$. The \mathcal{O}_7 and $\mathcal{O}_{9,10}$ are the electromagnetic penguin and the semileptonic operators, respectively, and $\mathcal{O}_{1,2}^p$, $\mathcal{O}_{3,\dots,6}$, and \mathcal{O}_8 are the “current-current”, “QCD-penguins” and “chromo-magnetic” operators, respectively, which require of an electromagnetic interaction to contribute to the $b \rightarrow s\ell\ell$ transition via “non-factorizable” corrections, in the language of QCD factorization [19]. The effects of new physics beyond the SM can be modeled by modifying the Wilson coefficients C_1, \dots, C_{10} and by supplementing the effective Hamiltonian with chirally-flipped ($b_{L(R)} \rightarrow b_{R(L)}$) versions of these operators $\mathcal{O}'_{7,\dots,10}$, and also four scalar and two tensor operators [47].¹

Among all the possible operators present in \mathcal{H}_{eff} , only the semileptonic ones,

$$\mathcal{O}_9^{(\prime)\ell} = \frac{\alpha_{\text{em}}}{4\pi} (\bar{s}\gamma^\mu P_{L(R)} b) (\bar{\ell}\gamma_\mu \ell), \quad \mathcal{O}_{10}^{(\prime)\ell} = \frac{\alpha_{\text{em}}}{4\pi} (\bar{s}\gamma^\mu P_{L(R)} b) (\bar{\ell}\gamma_\mu \gamma_5 \ell), \quad (5)$$

can explain the deficit observed in R_K . The current-current, QCD penguin and magnetic operators do not induce lepton-universality violation because they connect to the dilepton pair through a photon. Scalar and tensor Lorentz structures cannot explain R_K either if they stem from an UV completion of the SM manifesting at the electroweak scale as $SU(3)_c \times SU(2)_L \times U(1)_Y$ -invariant effective operators: Tensor operators with the particle content of the SM of the type $(\bar{Q}_L \sigma_{\mu\nu} d_R)(\bar{L}_L \sigma^{\mu\nu} \ell_R)$ are forbidden by conservation of hypercharge, whereas $(\bar{Q}_L \sigma_{\mu\nu} d_R)(\bar{\ell}_R \sigma^{\mu\nu} L_L)$ is identically equal to zero. On the other hand, out of the four possible scalar operators at low energies only two are independent, and these are found to be severely constrained by the $B_q \rightarrow \ell\ell$ decay rates so they cannot explain R_K either (see refs. [37, 38] for details).

In terms of the operators of the type (5), and expanding around the massless limit for the lepton the differential decay rate of the $B \rightarrow K\ell\ell$ process is [47]

$$\begin{aligned} \frac{d\Gamma_K}{dq^2} = & \mathcal{N}_K |\vec{k}|^3 f_+(q^2)^2 \left(\left| C_{10}^\ell + C_{10}^{\prime\ell} \right|^2 + \left| C_9^\ell + C_9^{\prime\ell} + 2 \frac{m_b}{m_B + m_K} C_7 \frac{f_T(q^2)}{f_+(q^2)} - 8\pi^2 h_K \right|^2 \right) \\ & + \mathcal{O}\left(\frac{m_\ell^4}{q^4}\right) + \frac{m_\ell^2}{m_B^2} \times \mathcal{O}(\alpha_s, \frac{q^2}{m_B^2} \times \frac{\Lambda}{m_b}), \end{aligned} \quad (6)$$

where $\Lambda \equiv \Lambda_{\text{QCD}}$, \vec{k} is the 3-momentum of the recoiling meson in the B -meson rest-frame, \mathcal{N}_K is a dimensionful normalization constant that drops out in the ratio R_K , $f_{+,T}(q^2)$ are $B \rightarrow K$ form factors and h_K encompasses the hadronic effects of the current-current, chromomagnetic and QCD penguin operators. It is clear from this equation that phase-space effects induced by the lepton masses are negligible as soon as $q^2 \gtrsim 1 \text{ GeV}^2$ and that the ratio of decay rates into muons and electrons must be very accurately equal to 1 (up to electromagnetic corrections [2]), and regardless of hadronic contributions since these are necessarily lepton-universal. Since, $C_{1,\dots,8}$ do not directly result in lepton-universality violation, any significant deficit from 1 in R_K must be then caused by non-universal NP contributions $\delta C_{9,10}^{(\prime)}$. Hence, taking into account that $C_9^{\text{SM}}(m_b) \simeq -C_{10}^{\text{SM}} = 4.27$, explaining the central value of the LHCb measurement in eq. (1) with muon-specific NP contributions would require [37, 38]

$$\delta C_9^{(\prime)\mu} \simeq -1, \quad \text{or} \quad \delta C_{10}^{(\prime)\mu} = +1, \quad (7)$$

¹ In the bottom-up approach followed in this paper one defines different “new-physics scenarios” by varying the values of these Wilson coefficients, without considering which could be the new degrees of freedom or specific UV completions of the SM producing them.

or a suitable combination of the two such as in the leptonic left-handed combination,

$$\delta C_L^\mu = \delta C_9^\mu = -\delta C_{10}^\mu = -0.5, \quad (8)$$

(or its chirally-flipped counterpart $\delta C_L^{\prime\mu} = \delta C_9^{\prime\mu} = -\delta C_{10}^{\prime\mu}$). Explaining the signal instead with electron-specific contributions would require the replacements $\delta C^e \simeq -\delta C^\mu$ in the scenarios above.

The dependence of the $\bar{B} \rightarrow \bar{K}^* \ell \ell$ rate on the Wilson coefficients is more involved due to the interplay between different helicity amplitudes in the rate. For instance one can express it as

$$\frac{d\Gamma_{\bar{K}^*}}{dq^2} = \frac{d\Gamma_\perp}{dq^2} + \frac{d\Gamma_0}{dq^2}, \quad (9)$$

where Γ_0 (Γ_\perp) corresponds to the decay rate into longitudinally or transversally polarized \bar{K}^* , and we define $F_L = \Gamma_0/\Gamma_{\bar{K}^*}$ as the longitudinal polarization fraction in the decay. Expanding the $\bar{B} \rightarrow \bar{K}^* \ell \ell$ rates around the massless limit of the lepton, one obtains

$$\frac{d\Gamma_0}{dq^2} = \mathcal{N}_{K^*0} |\vec{k}|^3 V_0(q^2)^2 \left(|C_{10}^\ell - C_{10}^{\prime\ell}|^2 + \left| C_9^\ell - C_9^{\prime\ell} + \frac{2m_b}{m_B} C_7 \frac{T_0(q^2)}{V_0(q^2)} - 8\pi^2 h_{K^*0} \right|^2 \right) + \mathcal{O}\left(\frac{m_\ell^2}{q^2}\right), \quad (10)$$

$$\begin{aligned} \frac{d\Gamma_\perp}{dq^2} &= \mathcal{N}_{K^*\perp} |\vec{k}| q^2 V_-(q^2)^2 \left(|C_{10}^\ell|^2 + |C_9^{\prime\ell}|^2 + |C_{10}^{\prime\ell}|^2 + \left| C_9^\ell + \frac{2m_b m_B}{q^2} C_7 \frac{T_-(q^2)}{V_-(q^2)} - 8\pi^2 h_{K^*\perp} \right|^2 \right) \\ &+ \mathcal{O}\left(\frac{m_\ell^2}{q^2}\right) + \mathcal{O}\left(\frac{\Lambda}{m_b}\right). \end{aligned} \quad (11)$$

In this formula $\mathcal{N}_{K^*0,\perp}$ are dimensionful constants, $V_{0,-}(q^2)$ and $T_{0,-}(q^2)$ are form factors in the helicity basis [25] and $h_{K^*0,\perp}$ describe the contributions from the four-quark and chromomagnetic operators much like h_K above. Furthermore, we have neglected the hadronic matrix elements giving the leading contributions in the SM to decays into positively polarized K^* (e.g. the form factors $V_+(q^2)$ and $T_+(q^2)$) because, in the large-recoil region (low q^2), they are suppressed by $\mathcal{O}(\Lambda/m_b)$ [25]. In the SM these corrections, as well as, in general, the hadronic uncertainties, largely cancel in the R_{K^*} ratios, formally appearing as $\mathcal{O}(m_\mu^2/q^2 \times \Lambda/m_b)$ terms that will be systematically included in our numerical analysis.

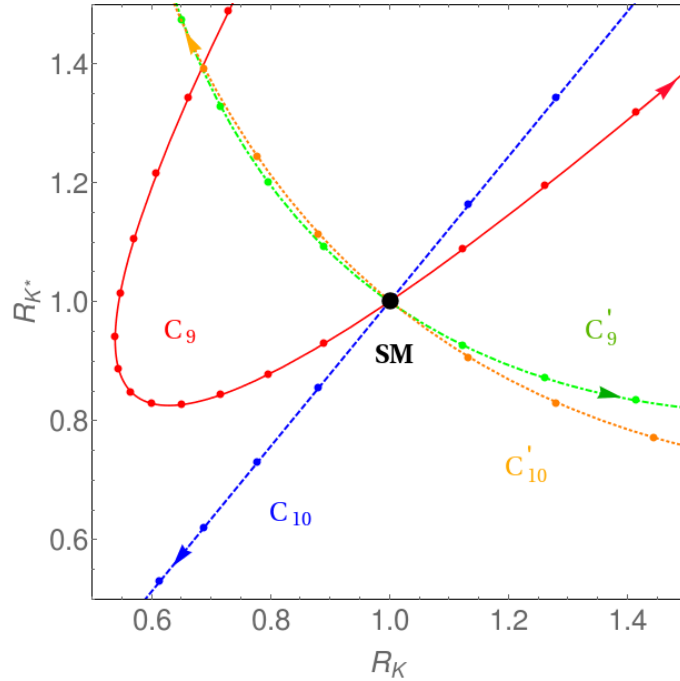


FIG. 1: R_K and R_{K^*} (in the $[1.1, 6]$ GeV^2 bin) parametric dependence on one Wilson coefficient at a time, for NP affecting only the muonic coefficients, where the nodes indicate steps of $\Delta(\delta C^\mu) = +0.5$ from the SM point and in the direction of the arrows. The red solid line shows the dependence on δC_9^μ , dashed blue line on δC_{10}^μ , green dot-dashed on $\delta C_9^{\prime\mu}$ and orange dotted on $\delta C_{10}^{\prime\mu}$.

The longitudinal contribution to the rate, eq. (10), is similar to the $B \rightarrow K\ell\ell$ one except that the chirally flipped operators interfere with the SM with a relative minus sign due to the different transformations under parity of the $B \rightarrow K$ and $B \rightarrow K^*$ hadronic matrix elements. In the transversal polarization, the interference of the chirally flipped operators with the SM is suppressed by the neglected Λ/m_b terms in eq. (11), so that their contributions will always increase Γ_\perp . Any scenario explaining the deficit in R_K via a destructive interference with the SM in eq. (6) with (small) negative values of $C'_{9,10}$, will necessarily produce a *surplus* in R_{K^*} .

Another interesting feature of the transversal rate is the destructive interference that occurs in the SM between \mathcal{O}_9 and \mathcal{O}_7 ($C_7(m_b) = -0.333$) whose contribution is the dominant one at low q^2 because of the pole of the virtual photon exchanged with the lepton pair. A negative contribution to C'_9 would then *increase* Γ_\perp , partially compensating for the deficit that the very same contribution would produce in Γ_0 . Thus, a C_9 scenario is not as efficient at reducing R_{K^*} at low q^2 as it is in R_K , or as compared to a contribution from \mathcal{O}_{10} , which would coherently reduce the three decay rates Γ_K , Γ_0 , and Γ_\perp .²

In Fig. 1 we show the parametric dependence of R_K and R_{K^*} (in the $[1.1, 6]$ GeV² bin) on one Wilson coefficient. The nodes indicate steps of $\Delta C^\mu = +0.5$ from the SM point and in the direction of the arrows, illustrating the patterns discussed in this section.

III. PREDICTIONS IN THE STANDARD MODEL AND IN SELECTED NEW-PHYSICS SCENARIOS

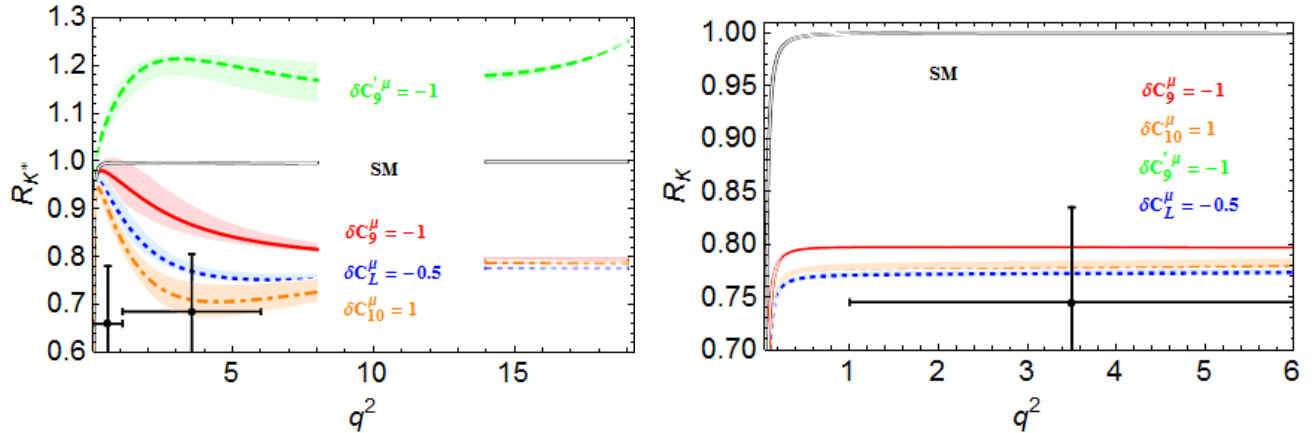


FIG. 2: Results for R_{K^*} and R_K in the SM and various NP scenarios as a function of the invariant mass of the lepton pair, q^2 . Solid gray line corresponds to the SM, solid red line to the scenario in which $\delta C_9^\mu = -1$, dot-dashed orange line to $\delta C_{10}^\mu = 1$, dashed green line to $\delta C_9^\mu = -1$ and blue dotted line to $\delta C_L^\mu = -0.5$. The shadings around each curve indicates our estimate of the hadronic uncertainties (see main text). We overlay the experimental LHCb results shown in black as points with error bars.

TABLE I: Results for binned observables in the SM and different NP scenarios using the approach described in ref. [29]. The errors are obtained with the gaussian method described in ref. [29] for the distributions of the hadronic parameters. The experimental results have been rounded conservatively by taking the larger side of the statistical error and adding the systematic in quadrature, and neglecting correlations. We show also predictions for the high q^2 bin.

Obs.	Expt.	SM	$\delta C_L^\mu = -0.5$	$\delta C_9^\mu = -1$	$\delta C_{10}^\mu = 1$	$\delta C_9^{\prime\mu} = -1$
R_K [1, 6] GeV ²	0.745 ± 0.090	$1.0004^{+0.0008}_{-0.0007}$	$0.773^{+0.003}_{-0.003}$	$0.797^{+0.002}_{-0.002}$	$0.778^{+0.007}_{-0.007}$	$0.796^{+0.002}_{-0.002}$
R_{K^*} [0.045, 1.1] GeV ²	0.66 ± 0.12	$0.920^{+0.007}_{-0.006}$	$0.88^{+0.01}_{-0.02}$	$0.91^{+0.01}_{-0.02}$	$0.862^{+0.016}_{-0.011}$	$0.98^{+0.03}_{-0.03}$
R_{K^*} [1.1, 6] GeV ²	0.685 ± 0.120	$0.996^{+0.002}_{-0.002}$	$0.78^{+0.02}_{-0.01}$	$0.87^{+0.04}_{-0.03}$	$0.73^{+0.03}_{-0.04}$	$1.20^{+0.02}_{-0.03}$
R_{K^*} [15, 19] GeV ²	—	$0.998^{+0.001}_{-0.001}$	$0.776^{+0.002}_{-0.002}$	$0.793^{+0.001}_{-0.001}$	$0.787^{+0.004}_{-0.004}$	$1.204^{+0.007}_{-0.008}$

In Fig. 2 and Tab. I we present predictions for the differential and binned lepton-universality ratios in the SM and in various benchmark NP scenarios of interest, compared to the experimental measurements by the LHCb. The NP scenarios coupling

² In this paper we will not consider new physics in $C_7^{(\prime)}$ that could contribute through these interference terms. These Wilson coefficients are very tightly constrained by the decay $B \rightarrow X_s \gamma$, the time dependent CP -asymmetry of $B \rightarrow K^* \gamma$ and the angular analysis of $B \rightarrow K^* e e$ at a very low q^2 [29, 48, 49].

selectively to the electrons produce very similar results to those of the muons replacing $\delta C_i^e \simeq -\delta C_i^\mu$. The calculations are performed following ref. [29] and where the errors are obtained with the gaussian method described there for the distributions of the hadronic parameters. The central values and uncertainties for the inputs are listed in Table II of ref. [29] except for the parametrizations describing the corrections to the heavy-quark limit, whose functional form and numerical values for the error intervals of the parameters are described in Sec. II-A of this reference. For R_K we extend to $B \rightarrow K\ell\ell$ decays the parametrization of power corrections put forward for $B \rightarrow K^*\ell\ell$ in ref. [25] and use input from light-cone sum rules [24] to fix the only form factor appearing in the heavy-quark limit [50] and to estimate the effects of the soft-gluon exchange in the charm-contribution to the decay (see [25, 29] for details). Uncertainties for the high q^2 region account only for the errors of the lattice calculation of the form factors [26] and we do not attempt to quantify the uncertainties of duality violations to the operator-product expansion treatment of the charm [20] implemented in our analysis. Let us stress again that in the SM these uncertainties almost cancel in the lepton universality ratios, as shown in our predictions in Tab. I, and are negligible as advertised. This is not longer true in presence of lepton-specific NP contributions, especially for the case of the R_{K^*} .³ It is important to stress that radiative electromagnetic corrections, which break lepton universality and can reach the $\gtrsim 2\%$ level at the level of the measured ratios [2], have not been included in our predictions.

The dependence on the Wilson coefficients of interest of R_K and R_{K^*} in the bins $[1, 6] \text{ GeV}^2$ and $[1.1, 6] \text{ GeV}^2$, respectively, as functions of the Wilson coefficients of the four semileptonic operators can be expressed as

$$\begin{aligned} \frac{\Gamma_K}{\Gamma_K^{\text{SM}}} &= (2.9438 (|C_9 + C'_9|^2 + |C_{10} + C'_{10}|^2) - 2\text{Re}[(C_9 + C'_9)(0.8152 + i 0.0892)] + 0.2298) 10^{-2}, \\ \frac{\Gamma_{K^*}}{\Gamma_{K^*}^{\text{SM}}} &= (2.420 (|C_9 - C'_9|^2 + |C_{10} - C'_{10}|^2) - 2\text{Re}[(C_9 - C'_9)(2.021 + i 0.188)] + 1.710 \\ &\quad + 1.166 (|C_9|^2 + |C_{10}|^2 + |C'_9|^2 + |C'_{10}|^2) - 2\text{Re}[C_9(5.255 + i 0.239)] + 29.948) 10^{-2}, \end{aligned} \quad (12)$$

where the numerical coefficients have been obtained using ref. [29] at a scale $\mu = 4.65 \text{ GeV}$. These formulas give results on the ratios which are accurate at the $\sim 1\%$ level (which is better than the hadronic uncertainties) when compared to the exact numerical calculation and can be directly used to obtain predictions for NP defects in muons or in electrons.

In light of the discussion above and given the *deficits* observed in both R_K and R_{K^*} we conclude that the primed operators $\mathcal{O}'_{9,10}$ are disfavored by the data. Henceforth we will focus only on the analysis of the operators \mathcal{O}_9 and \mathcal{O}_{10} .

IV. FITS TO $R_{K^{(*)}}$ AND OTHER $b \rightarrow s\ell\ell$ DATA

In this section we assess the compatibility with the SM of lepton-universality-violating and -conserving rare B -decay measurements, and perform frequentist fits to (NP values of) Wilson coefficients in the weak Hamiltonian. In all cases, theoretical uncertainties are modeled by adding a “theory term” to the χ^2 ,

$$\tilde{\chi}^2(\vec{C}, \vec{y}) = \chi_{\text{exp}}^2(\vec{C}, \vec{y}) + \chi_{\text{th}}^2(\vec{y}). \quad (13)$$

Here $\chi_{\text{exp}}^2(\vec{C}, \vec{y})$ is constructed in the usual way out of the experimental measurements considered, and the theoretical expressions for them in terms of a vector of Wilson coefficients \vec{C} included in a given fit, and the 27-component vector \vec{y} of hadronic parameters that enter in the model-independent description of the $B \rightarrow K^*\ell\ell$ [25, 29]. The theory term is taken in gaussian form

$$\chi_{\text{th}}^2(\vec{y}) = \sum_i \left(\frac{y_i - \bar{y}_i}{\delta y_i} \right)^2, \quad (14)$$

where \bar{y}_i are the central values of the theory parameters and δy_i their estimated uncertainties, which we assume to be fully uncorrelated [29].⁴

Once it is in this form, we treat the y_i as nuisance parameters and construct a profile χ^2 that depends on the Wilson coefficients only,

$$\chi^2(\vec{C}) = \min_{\vec{y}} \tilde{\chi}^2(\vec{C}, \vec{y}), \quad (15)$$

³ It is interesting to note, though, that effects in $R_{K^{(*)}}$ of lepton-specific contributions to δC_9^ℓ should be enhanced around the mass of resonances (charmoniums at high- q^2 or the ϕ at low- q^2) because of the interference effects.

⁴ Theoretical uncertainties for R_K are always very small compared to the experimental errors in all scenarios considered (see Fig. 2 and Tab. I) and are neglected in our analysis.

from which we determine frequentist confidence level intervals and contours for the Wilson coefficients. The construction here is nothing but the Rfit method [51] with gaussian theory errors instead of parameter ranges.

A. Fits only to R_K and R_{K^*}

We begin by considering R_K and R_{K^*} alone. Setting the Wilson coefficients to their SM values, we obtain $\chi_{\min, \text{SM}}^2 = 19.51$ 3 degrees of freedom (d.o.f.), corresponding to a p -value of 2.1×10^{-4} or a 3.7σ deviation. It must be stressed that the significance of this evidence for new physics in lepton-universality ratios alone is fully dominated by experimental statistical errors, with hadronic uncertainties (the y_i -parameters) playing almost no role, due to the exceptional cleanliness of the observables. Nonetheless, in our fit we include the theoretical errors of R_{K^*} at low q^2 and investigate below the robustness of our fits against variations of the theoretical error ranges.

We next show that a good fit is obtained by allowing for lepton-specific contributions δC_9^ℓ and δC_{10}^ℓ . In Table II and Figure 3 we display the results of one- and two-dimensional fits of muon-specific NP Wilson coefficient values δC_9^μ and δC_{10}^μ .

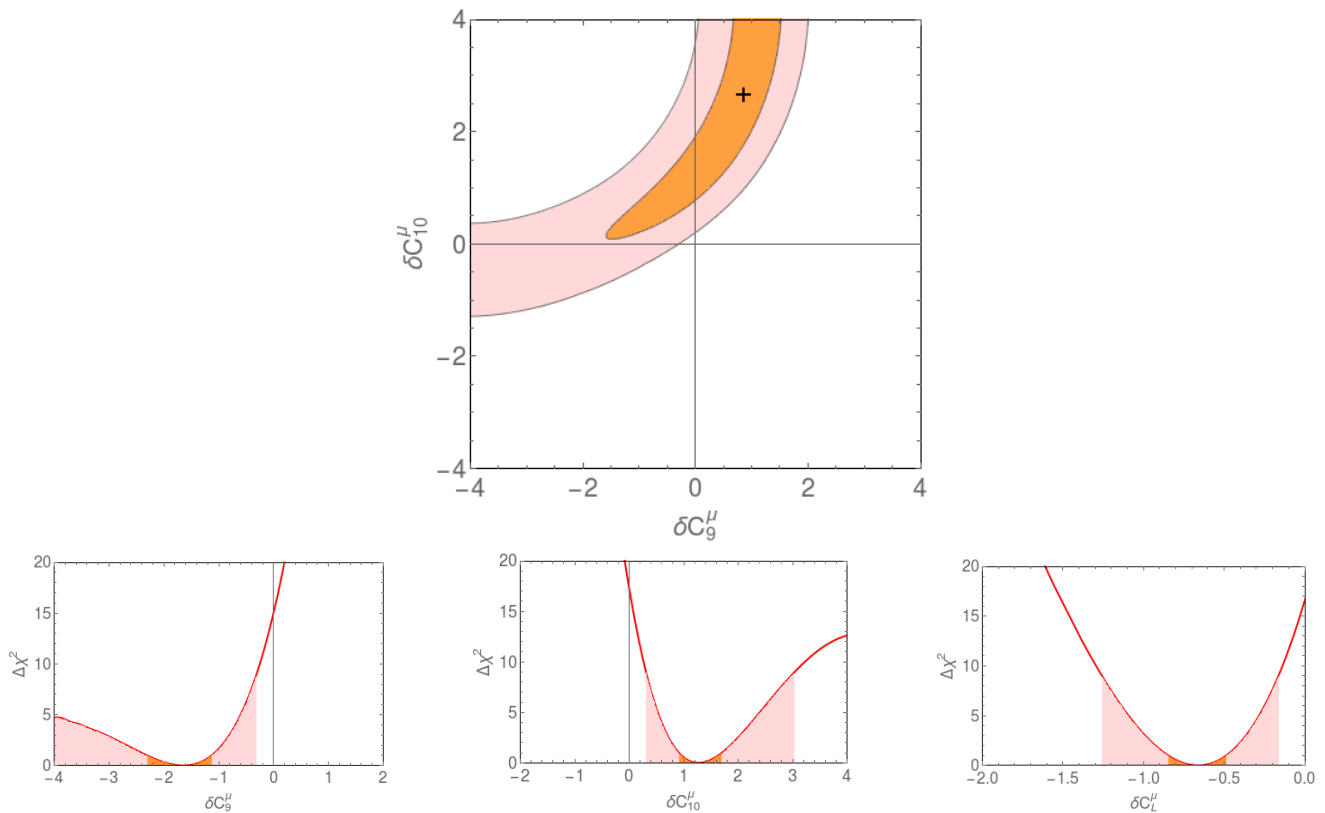


FIG. 3: The top panel shows the result of a best fit to a model that includes muon-specific NP Wilson coefficients δC_9^μ and δC_{10}^μ . The cross indicates the position of the minimum. The first two graphs in the bottom row give the χ^2 distribution projected onto each Wilson coefficient, while the third one is projected onto the difference $\delta C_L^\mu = \delta C_9^\mu - \delta C_{10}^\mu$. Ranges in orange and light red correspond to 1 and 3 intervals of Wilson coefficients, respectively. ($\Delta\chi^2 = 1(9)$ for $1\sigma(3\sigma)$ in the 1-parameter cases, $\Delta\chi^2 = 2.3(11.83)$ for $1\sigma(3\sigma)$ in the 2-parameter fit.)

Good to excellent fits are obtained in one-parameter scenarios where only δC_{10}^μ , $\delta C_L^\mu = \delta C_9^\mu = -\delta C_{10}^\mu$, or δC_9^μ are nonzero, as well as in the two-parameter scenario. The largest p -value (best fit) is obtained in the pure C_{10}^μ -case, though the differences are not large. We next consider $\Delta\chi^2 = \chi^2 - \chi_{\min}^2$ and use it to compute the significance at which the SM point (origin) is excluded (often called “pull”), and to construct frequentist confidence regions. In each of the four scenarios, the SM point (origin) is excluded at 4σ confidence, or close to it (see Table II, where we also display best-fit values and confidence intervals for the parameters (in the two-dimensional case, these are obtained by minimising $\Delta\chi^2$ over the other parameter).

Instead of considering muon-specific effects, we could have assumed an electron-specific effect, or a combination. In the former case, essentially the signs of the fitted Wilson coefficients are reversed, if only the LUV observables are considered.

TABLE II: Best fit values, goodness of fit, p -value, SM exclusion level (pull), and confidence intervals for fits of single or pairs of Wilson coefficients, to R_K and R_{K^*} data. For the one-dimensional case, we show that the 1σ and 3σ confidence intervals, while for the two-dimensional case we show the one-sigma intervals for the two parameters instead.

Coeff.	best fit	χ_{\min}^2	p -value	SM exclusion [σ]	1σ range	3σ range
δC_9^μ	-1.64	4.52	0.104	3.87	[-2.31,-1.13]	[<-4, -0.31]
δC_{10}^μ	1.27	2.24	0.326	4.15	[0.91,1.70]	[0.31,3.04]
δC_L^μ	-0.66	2.93	0.231	4.07	[-0.85,-0.49]	[-1.26,-0.16]
Coeff.	best fit	χ_{\min}^2	p -value	SM exclusion [σ]	parameter ranges	
$(\delta C_9^\mu, \delta C_{10}^\mu)$	(0.85, 2.69)	1.99	0.158	3.78	$C_9^\mu \in [-0.71, 1.38]$	$C_{10}^\mu \in [0.61, >4]$

B. Fits to R_K, R_{K^*} and $B_s \rightarrow \mu\mu$

We now add $\overline{\text{BR}}(B_s \rightarrow \mu\mu)$ to the data set.⁵ It is theoretically very clean with NNLO QCD and NLO electroweak corrections known [53], and the sole hadronic parameter, the decay constant f_{B_s} , having been precisely computed by different lattice QCD collaborations [54]. To simplify the fit, we consider the ratio

$$R = \frac{\overline{\text{BR}}(B_s \rightarrow \mu\mu)}{\overline{\text{BR}}(B_s \rightarrow \mu\mu)^{\text{SM}}} = \left| \frac{C_{10}^\mu}{C_{10}^{\text{SM}}} \right|^2, \quad (16)$$

where we have neglected the contributions of scalar operators. Among the set (C_9^ℓ, C_{10}^ℓ) , this branching fraction only depends on the coefficient C_{10}^μ , such that it is natural to add it to the fit of muon-specific Wilson coefficients. As experimental value for R we employ the combination obtained in ref. [55], $R^{\text{exp}} = 0.83(16)$, where the results from CMS and LHCb including run I and run II data have been averaged. The error includes, in quadrature, the theory uncertainty on the SM rate, which is small compared to the experimental ones.

Including R increases the SM p -value marginally to $3.7 \cdot 10^{-4}$ (3.56σ). We next perform the same fits as in the previous subsection, but to the extended data set. The results are shown in Tab. III and, for the fit of $(\delta C_9^\mu, \delta C_{10}^\mu)$ fit, in Fig. 4.

TABLE III: As in Table II but in fits to R_K, R_{K^*} and $B_s \rightarrow \mu\mu$ data.

Coeff.	best fit	χ_{\min}^2	p -value	SM exclusion [σ]	1σ range	3σ range
δC_9^μ	-1.64	5.65	0.130	3.87	[-2.31, -1.12]	[<-4, -0.31]
δC_{10}^μ	0.91	4.98	0.173	3.96	[0.66, 1.18]	[0.20, 1.85]
δC_L^μ	-0.61	3.36	0.339	4.16	[-0.78, -0.46]	[-1.14, -0.16]
Coeff.	best fit	χ_{\min}^2	p -value	SM exclusion [σ]	parameter ranges	
$(\delta C_9^\mu, \delta C_{10}^\mu)$	(-0.76, 0.54)	3.31	0.191	3.76	$C_9^\mu \in [-1.50, -0.16]$	$C_{10}^\mu \in [0.18, 0.92]$

Again, all four scenarios considered provide good fits. The main impact on the two-parameter fit is that the allowed region is narrowed down considerably, with large positive correlated values of δC_9^μ and δC_{10}^μ no longer allowed. We note, in particular, that the combination of $C_L^\mu = \frac{1}{2}(C_9^\mu - C_{10}^\mu)$ is nonzero at more than 4σ significance, and is relatively well determined by the LUV data set plus $B_s \rightarrow \mu\mu$ alone, irrespective of and in contradistinction from the value of $C_R^\mu = \frac{1}{2}(C_9^\mu + C_{10}^\mu)$, which is consistent with zero and poorly constrained.

C. Fits to $R_K, R_{K^*}, B_s \rightarrow \mu\mu$ and $B \rightarrow K^* \ell\ell$ data

We now include in the fits all measurements of the angular distribution in $B \rightarrow K^* \mu\mu$ by LHCb, ATLAS, CMS, and Belle in the low- q^2 region $q^2 \lesssim 6 \text{ GeV}^2$ (except for lepton-universality differences measured by Belle, for which we do include the [4, 8] GeV^2 bin). The reason for this restriction is that we can then reasonably estimate the size of the hadronic uncertainties. As advertised above, we will later quantify the robustness of our conclusions with respect to the size of the theoretical errors. The precise dataset comprises

⁵ The overline refers to the fact that the experiments access the time-integrated branching ratio, which depends on the details of $B_s \bar{B}_s$ mixing [52].

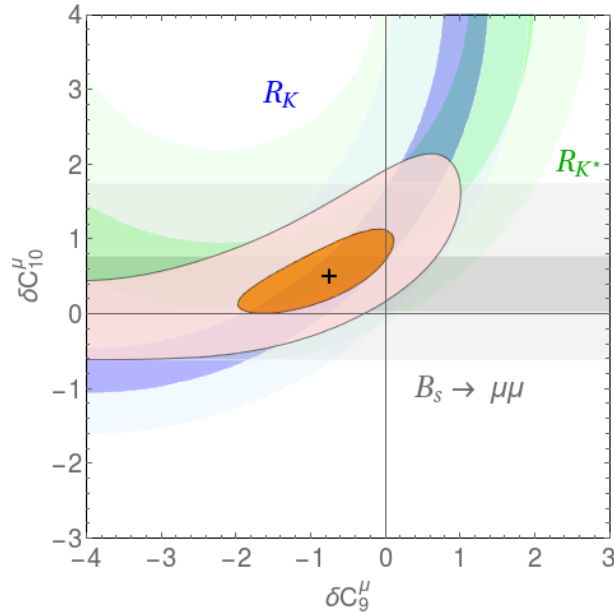


FIG. 4: Contours at 1σ and 3σ level in the $(\delta C_9^\mu, \delta C_{10}^\mu)$ plane, in solid lines and orange and light-red colors, for the fit to R_K , R_{K^*} and $\overline{\text{BR}}(B_s \rightarrow \mu\mu)$. We also show the 1σ and 3σ constraints given individually by R_K , R_{K^*} in the $[1.1, 6]$ GeV^2 bin and $\overline{\text{BR}}(B_s \rightarrow \mu\mu)$ using blue, green and gray contours, respectively. The cross indicates the position of the minimum.

- **LHCb:** The 32 measurements of the CP -averaged angular observables F_L , P_1 , P_2 , P_3 , P_4 , P_5 , P_6 , P_8 in the bins $[0.1, 0.98]$ GeV^2 , $[1.1, 2.5]$ GeV^2 , $[2.5, 4]$ GeV^2 and $[4, 6]$ GeV^2 [9] including, inside of each bin, the published correlations among the observables.
- **ATLAS:** The 18 measurements of the CP -averaged angular observables F_L , P_1 , P_4 , P_5 , P_6 , P_8 in the bins $[0.04, 2]$ GeV^2 , $[2, 4]$ GeV^2 , $[4, 6]$ GeV^2 reported in Moriond EW 2017 [11]. Correlations of this data are not public and are neglected.
- **CMS:** The 6 measurements of the CP -averaged angular observables P_1 and P_5 in the bins $[1, 2]$ GeV^2 , $[2, 4.3]$ GeV^2 , $[4.3, 6]$ GeV^2 reported in Moriond EW 2017 [12]. Correlations of this data are not public and are neglected.
- **Belle:** The 4 measurements of the CP -averaged lepton universality differences of angular observables Q_4 and Q_5 in the bins $[1, 4]$ GeV^2 and $[4, 8]$ GeV^2 [10]. Correlations of this data are not public and are neglected.

In addition, we include in the fit the $\text{BR}(B \rightarrow K^*\gamma)$ [56–60] which provides an important constraint to a hadronic form factor in the fit [29]. Including the measurements of R_K , R_{K^*} and $\overline{\text{BR}}(B_s \rightarrow \mu\mu)$, the total number of measurements in the fit is 65.

The resulting $\chi_{\min, \text{SM}}^2$ -value is 81.1 [65 d.o.f.], corresponding to a p -value of 0.086. Note that this is considerably larger than before—adding the many angular observables, the significance of the anomalies has decreased. Each of the four models we consider provides an excellent fit, once the full data set is considered. At the same time, the significance of the SM exclusion in three of the four fits is above 4σ ; we show fit results in Table IV. The main impact on the fits is to narrow down the C_9^μ range

TABLE IV: Same as Table III, but with $\text{BR}(B \rightarrow K^*\gamma)$, the $B \rightarrow K^*\mu\mu$ angular distribution and Q_i observables added to the data set.

Coeff.	best fit	χ_{\min}^2	p -value	SM exclusion [σ]	1σ range	3σ range
δC_9^μ	-1.37	61.98 [64 dof]	0.548	4.37	[-1.70, -1.03]	[-2.41, -0.41]
δC_{10}^μ	0.60	71.72 [64 dof]	0.237	3.06	[0.40, 0.82]	[-0.01, 1.28]
δC_L^μ	-0.59	63.62 [64 dof]	0.490	4.18	[-0.74, -0.44]	[-1.05, -0.16]
Coeff.	best fit	χ_{\min}^2	p -value	SM exclusion [σ]	parameter ranges	
$(\delta C_9^\mu, \delta C_{10}^\mu)$	(-1.15, 0.28)	60.33 [63 dof]	0.572	4.17	$C_9^\mu \in [-1.54, -0.81]$	$C_{10}^\mu \in [0.06, 0.50]$

further, excluding positive values at high confidence. Note that the axes of the, approximately elliptic, allowed region in the two-parameter fit are nearly aligned with the C_L^μ and C_R^μ directions, in such a fashion that C_L^μ is again nonzero at more than 4σ confidence, while C_R^μ is more or less consistent with zero, and much less well determined.

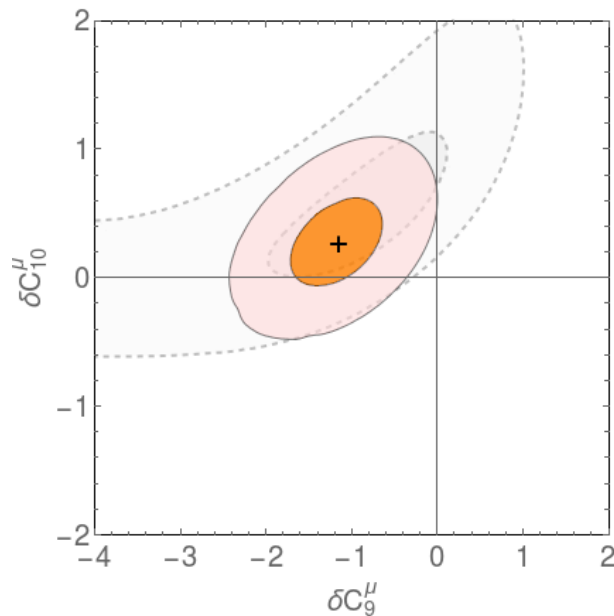


FIG. 5: Contours at 1σ and 3σ level in the $(\delta C_9^\mu, \delta C_{10}^\mu)$ plane, in solid lines and orange and light-red colors, for the fit to LUV data, $\overline{\text{BR}}(B_s \rightarrow \ell\ell)$, $\text{BR}(B \rightarrow K^*\gamma)$, the $B \rightarrow K^*\mu\mu$ angular distribution, the Q_i observables, and the $B \rightarrow K^*e^+e^-$ angular observables in the ultralow bin. The cross indicates the position of the minimum. Excluding the latter electronic data produces a very similar fit. Underneath, and for comparison purposes, we show in gray colors and dashed lines the 1σ and 3σ regions for the fit to only LUV data and $\overline{\text{BR}}(B_s \rightarrow \ell\ell)$ described in the Sec. IV B and plotted in Fig. 4.

Finally, we consider the measurements of $B \rightarrow K^*e^+e^-$ performed by LHCb, namely of the branching fraction [61], as well as of four angular observables [48] with a reduced form-factor dependence similarly to the muonic case. A fit including the resulting 70 measurements is shown in Figure 5. Including or omitting the electron data has only a minimal impact on the fit and statistical tests.

D. Robustness of fit with respect to hadronic uncertainties

We investigate the robustness of our fits to the theoretical uncertainties of the $B \rightarrow K^*\mu\mu$ amplitude, which can affect considerably the predictions of the angular analysis and, therefore, the tensions of the SM with the data. In order to do so, we perform a scan of the variable x , that is a factor by which we multiply all the uncertainty ranges of the theoretical parameters in eq. (14), in the range $x \in [0.5, 3]$. At each x , we calculate the variation of the $\chi_{\text{d.o.f.}}^2$ with respect to x in the SM in the fit to only R_K , R_{K^*} and $\overline{\text{BR}}(B_s \rightarrow \mu\mu)$.⁶ The results are shown in Fig. 6 by the blue solid curve, which demonstrates the stability, with respect to the hadronic uncertainties in the semileptonic decays, of the fits to the lepton-universality ratios. This is just a consequence of the cancellations of hadronic uncertainties in the ratios discussed in previous sections. For illustrative purposes, we compare with the fit in which we also include the 61 measurements of observables in the angular distribution of $B \rightarrow K^*\mu\mu$ and the radiative $B \rightarrow K^*\gamma$ decay, which shows a much stronger sensitivity, as expected. A more careful treatment of hadronic uncertainties and their impact in the interpretation and analysis of the robustness of the global fits is left for future studies.

E. Beyond muon-specific lepton nonuniversality

As already noted, our choice to focus on new physics in muonic Wilson coefficients C_9^μ, C_{10}^μ was far from mandatory. As an example of a more general scenario that can accommodate the data, in the left panel of Figure 7, we show a two-parameter fits of C_L^μ and C_L^e , to LUV data and $B_s \rightarrow \mu^+\mu^-$ and the full data set. In both cases, a high degree of degeneracy is seen, and pure C_L^e fits the data nearly as well as C_L^μ .

⁶ We do not modify the value of f_{B_s} which is obtained from the FLAG average of lattice QCD calculations [54].

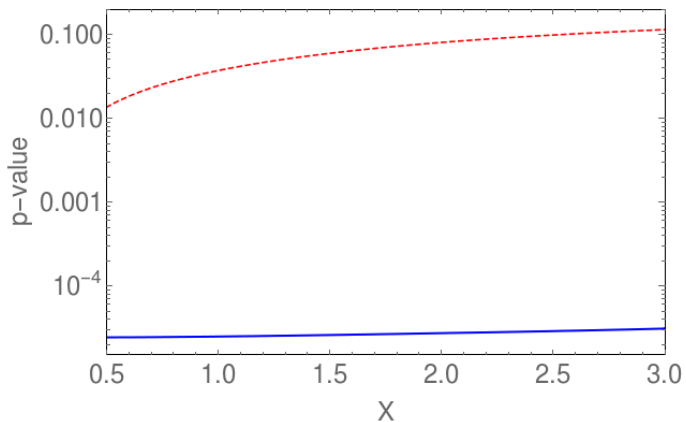


FIG. 6: *Robustness of fit*: Plot of the p -values of the SM as a function of x and in two different fits: Solid (Blue) line represents the fit to the R_K and R_{K^*} ratios and $B_s \rightarrow \mu\mu$ and the dashed (red) line represents the global fit including the $B \rightarrow K^* \mu\mu$ angular observables. The variable x is a factor by which we multiply all the uncertainty ranges of the theoretical parameters in eq. (14).

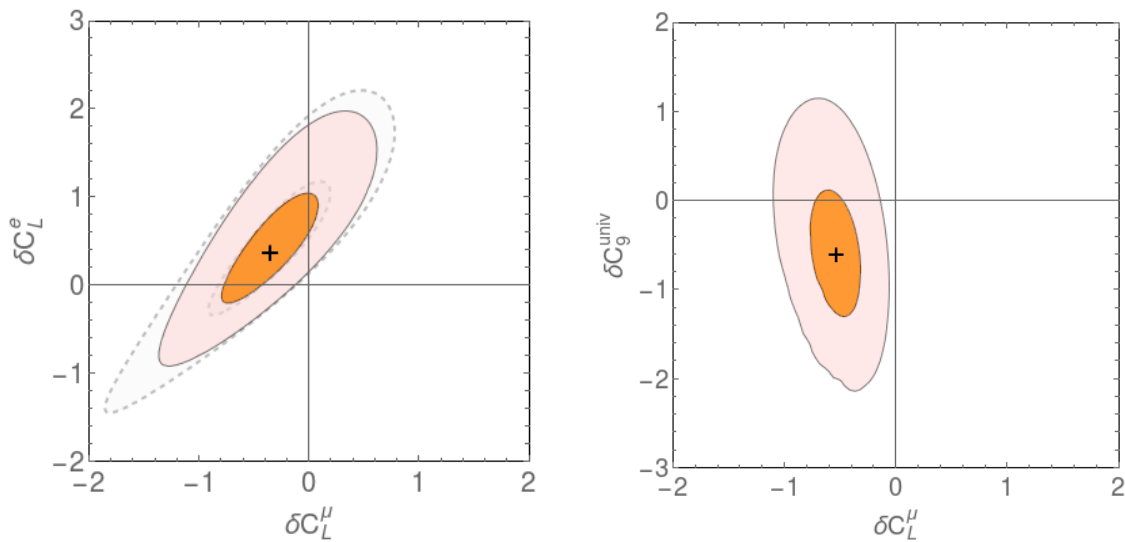


FIG. 7: *Left panel*: Two-parameter fit to C_L^μ and C_L^e where the gray regions and dashed contours include only R_K , R_{K^*} and $B_s \rightarrow \mu\mu$. The overlaid orange and light-red colored regions, enclosed by solid lines, represent the 1σ and 3σ bounds including the full data set. *Right panel*: Two-parameter fit to $C_9^e = C_9^\mu = C_9^{\text{univ}}$ and C_L^μ where we only show the 1σ and 3σ regions for the fit to the full data set. The crosses indicate the positions of the minima.

In the right panel of Figure 7 we consider instead a two-parameter scenario with a muon-specific Wilson coefficient C_L^μ and a lepton-flavour-universal coefficient $C_9^\mu = C_9^e = C_9$. Such a universal coefficient generically expected to be generated in BSM scenario at the one-loop level through penguin diagrams. One particular realisation is the “charming BSM scenario” of [62]. In fact, this “semi-universal” scenario fits the data minimally better the pure- C_L^μ ($p = 62\%$ versus $p = 60\%$). This preference for an extra C_9 effect can be understood as a consequence of the $B \rightarrow K^* \mu^+ \mu^-$ angular distribution measurements (particularly the P_5' term); because the $B \rightarrow K^* e^+ e^-$ measurements are much less precise and only cover $q^2 < 1.12 \text{ GeV}^2$, the data do not require this to be muon-specific. The preference for an extra, possibly universal, C_9^{univ} effect would increase with more optimistic error estimates on B -decay form factors that are sometimes made in the literature.

V. PRECISION PROBES OF A LEPTON-NONUNIVERSAL C_{10}

As shown above, low values of R_K^* at small dilepton mass, as suggested by the new LHCb measurements, require a modification of C_{10}^μ . However, the value of C_{10}^μ is poorly determined by the global fit: while the combination $C_L^\mu = (C_9^\mu - C_{10}^\mu)/2$ is already well determined and significantly different from zero, the combination $C_R^\mu = (C_9^\mu + C_{10}^\mu)/2$ is poorly constrained.

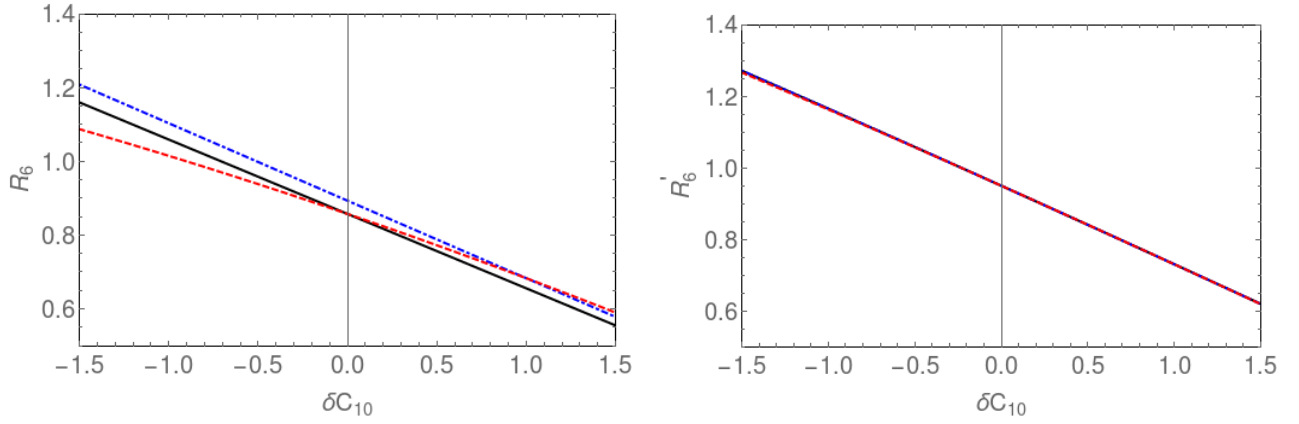


FIG. 8: Studies of sensitivity of the new precision probes R_6 , Eq. (18), and R'_6 , Eq. (19), to NP scenarios. *Left panel:* $R_6[0.045, 1.1]$ GeV² as a function of δC_{10} for different values of δC_9 : $\delta C_9 = 0$ (black solid), $\delta C_9 = -\delta C_{10}$ (red dashed), $\delta C_9 = -1$ (blue dot-dashed). *Right panel:* Same for $R'_6[0.045, 1.1]$ GeV².

Breaking the degeneracy between C_9^μ and C_{10}^μ will be a key requirement for identifying the dynamics underlying the NP signals. Currently, the most precise selective probe of the coefficient C_{10}^μ is the $B_s \rightarrow \mu^+ \mu^-$ branching fraction, but this suffers from low statistics. In this section we describe observables which are selectively sensitive to a lepton-nonuniversal C_{10} effect at a (theoretical) precision better than the percent level. They are sensitive to C_{10}^μ as well as C_{10}^e .

The starting point is the observation that the angular distribution in $B \rightarrow K^* \ell^+ \ell^-$ contains a single term proportional to C_{10} , commonly called I_6 , due to vector-axial-vector interference and responsible for the lepton forward-backward asymmetry. In terms of the helicity amplitudes,

$$I_6^{(\ell)} = N C_{10}^\ell q^2 \beta_\ell^2(q^2) |\vec{k}| \left(\text{Re}[H_{V-}^{(\ell)}(q^2)] V_-(q^2) + \text{Re}[H_{V+}^{(\ell)}(q^2)] \frac{H_{A+}^{(\ell)}(q^2)}{C_{10}^\ell} \right), \quad (17)$$

where N is a q^2 -independent normalisation, and $\beta_\ell^2 = 1 - 4m_\ell^2/q^2$ is the velocity-squared of the lepton in the dilepton rest frame (equal to one for electrons, for practical purposes). As shown in [25, 29], the amplitude H_{V+} is suppressed relative to H_{V-} by $q^2 \Lambda/m_B^3$ at small q^2 -values. Moreover, if the disfavoured Wilson coefficients $C_9^{\prime\ell}$ and $C_{10}^{\prime\ell}$ are neglected, $H_{A+}^{(\ell)} = C_{10}^\ell V_+$ is itself suppressed by one power of Λ/m_B in the heavy-quark limit. The second term hence gives at most a one-percent contribution below $q^2 = 1$ GeV² (but will be kept in our numerics).

Following [29], we define

$$R_6[a, b] = \frac{\int_a^b \Sigma_6^\mu dq^2}{\int_a^b \Sigma_6^e dq^2} \approx \frac{C_{10}^\mu}{C_{10}^e} \times \frac{\int_a^b |\vec{k}| q^2 \beta_\mu^2 \text{Re}[H_{V-}^{(\mu)}(q^2)] V_-(q^2)}{\int_a^b |\vec{k}| q^2 \text{Re}[H_{V-}^{(e)}(q^2)] V_-(q^2)}, \quad (18)$$

where Σ_6 is the CP-average of I_6 . The sensitivity of R_6 to deviations from C_{10}^μ/C_{10}^e from one is evident from the direct proportionality exhibited in (18). It was noted in [29] but not quantified. Moreover, the constant of proportionality—the ratio of integrals—differs from one only through the exactly known velocity-factor β_μ^2 and possible lepton-flavour-universality violation in H_{V-} . The only source of such lepton-flavour-nonuniversality would be a lepton-nonuniversal C_9^ℓ . Due to the dominance of the photon pole at small q^2 , for $|C_9^{\text{NP}}| \lesssim 1$ the resulting modification of H_{V-} is at the 5% level at $q^2 = 1$ GeV² and drops roughly linearly with q^2 below. Since Σ_6 is rather flat in q^2 below 1 GeV² (see Figure 6 in [25]), we conclude that the impact of NP effects in C_9^{NP} in $R_6[0.045, 1.1]$ GeV² is at most 2 – 3%. Moreover, this small effect is calculable with $\mathcal{O}(10 - 20\%)$ relative accuracy in the heavy-quark expansion. As a result, if $\delta C_{10}^e = 0$ then R_6 can theoretically determine δC_{10}^μ to an (absolute) accuracy of about 0.13 irrespective of the value of δC_9^ℓ . Below that level, R_6 still probes a combination of (mainly) δC_{10}^ℓ and δC_9^ℓ , which may still be useful in disentangling the two in the context of a global fit.

Figure 8 shows R_6 for the bin $[0.045, 1.1]$ GeV² as a function of C_{10}^μ for three scenarios differing in δC_9 . The sensitivity to δC_{10}^μ is evident from the slope and the narrowness of the bands in the figure, while the near-degeneracy of the three bands illustrates the insensitivity to δC_9^ℓ . Numerical values are given in Table V. They corroborate the preceding discussion and show that R_6 can clearly discriminate between the two benchmarks that remain viable in the light of the R_{K^*} measurements.

From an experimental perspective, R_6 may benefit from cancellations of certain systematics in the ratio, and from the fact that both numerator and denominator are rather flat in q^2 , which reduces the impact of energy-resolution uncertainties. Alternatively,

Obs.	SM	$\delta C_L^\mu = -0.5$	$\delta C_9^\mu = -1$	$\delta C_{10}^\mu = 1$	$\delta C_9^{\prime\mu} = -1$
$R_6[0.045, 1.1] \text{ GeV}^2$	$0.8571_{-0.0012}^{+0.0021}$	$0.7721_{-0.0014}^{+0.0006}$	$0.8930_{-0.0047}^{+0.0016}$	$0.6555_{-0.0007}^{+0.0016}$	$0.8570_{-0.0011}^{+0.0021}$
$\bar{R}_6[0.045, 1.1] \text{ GeV}^2$	$0.932_{-0.005}^{+0.007}$	$0.877_{-0.016}^{+0.010}$	$0.985_{-0.019}^{+0.008}$	$0.761_{-0.013}^{+0.010}$	$0.877_{-0.018}^{+0.030}$
$R'_6[0.034, 1.1] \text{ GeV}^2$	$0.9494_{-0.0006}^{+0.0005}$	$0.8403_{-0.0014}^{+0.0006}$	$0.9494_{-0.0014}^{+0.0004}$	$0.7300_{-0.0013}^{+0.0004}$	$0.948_{-0.003}^{+0.003}$
$Q_2[0.045, 1.1] \text{ GeV}^2$	$-0.0081_{-0.0005}^{+0.0012}$	$-0.026_{-0.002}^{+0.004}$	$-0.0081_{-0.0005}^{+0.0012}$	$-0.043_{-0.003}^{+0.006}$	$-0.008_{-0.001}^{+0.001}$

TABLE V: Predictions for the C_{10} analyzers R_6 , \bar{R}_6 , and R'_6 for the four benchmark scenarios consistent with the R_K measurement. The observable Q_2 is also shown, for comparison.

one may consider the following two observables, closely related to R_6 :

$$\bar{R}_6[a, b] = \frac{\int_a^b A_{FB}^\mu}{\int_a^b A_{FB}^e} = R_6[a, b]/R_{K^*}[a, b], \quad R'_6 = \langle P_2^{(\mu)} \rangle / \langle P_2^{(e)} \rangle, \quad (19)$$

where A_{FB} is the forward-backward asymmetry and P_2 is the corresponding ‘‘optimized observable’’ defined in ref. [63]. For example, \bar{R}_6 has numerator and denominator normalised to the respective integrated decay rate, such that a double ratio with $\Gamma(J/\psi\mu\mu)/\Gamma(J/\psi ee)$ may be considered, similarly to the R_K and R_{K^*} measurements. R_6 , \bar{R}_6 , and R'_6 are theoretically equally clean and have the same C_{10}^μ/C_{10}^e analyzing power as R_6 . The extreme insensitivity of R'_6 to the values of C_9^ℓ displayed in **V** and Fig. 8 is remarkable and turns these observables into the optimal analyzer of lepton nonuniversality in C_{10}^ℓ . However, the relatively larger sensitivity to C_9^ℓ in \bar{R}_6 relative to R'_6 is strongly correlated with that in R_{K^*} , such that a joint measurement of R_{K^*} and \bar{R}_6 can still determine C_{10}^μ precisely. By contrast, the observable Q_2 defined in [42] is sensitive to form factor ratios. It is a clean null test of lepton flavour universality, but does not provide a similarly precision determination of its violation, cf the Table.

In consequence, the choice among R_6 , \bar{R}_6 , and R'_6 should be guided by what minimizes experimental systematics. Most excitingly, a useful determination of each of these should be possible with existing data, both at LHCb and Belle. We illustrate this in Fig. 9 with the impact in the (C_9^μ, C_{10}^μ) -plane of a hypothetical measurement of $R'_6 = 0.80(5)$ in the bin $[0.045, 1.1] \text{ GeV}^2$, shown together with the result of the fit to R_K and R_{K^*} and the combined result. We end by noting that we have not considered in our discussion of these new observables the effect of the electromagnetic radiative corrections, which can be more severe for the ultralow bin. However, as discussed in [2] these can be minimized by choosing a more suitable bin starting at 0.1 GeV^2 , for which all the conclusions above will still apply.

VI. CONCLUSIONS

In this paper we have analysed the deficits, with respect to the Standard-Model expectations, of the lepton-universality ratios R_{K^*} recently measured by the LHCb. We first described the structure of the new-physics contributions to the $B \rightarrow K\ell\ell$ and $B \rightarrow K^*\ell\ell$ rates and the resulting correlations induced between R_K and R_{K^*} . We then presented the predictions of R_{K^*} in the bins of interest for the SM and in benchmark scenarios of new physics using a model-independent approach for the description of the $B \rightarrow K^*\ell\ell$ amplitude. The cleanliness of these observables, with respect to hadronic uncertainties, is discussed and demonstrated numerically. Furthermore, we provide numerical formulas for the dependence of $R_{K^{(*)}}$ as functions of the Wilson coefficients which can be useful for phenomenological applications. Finally, we discarded the primed operators $\mathcal{O}'_{9(10)}^\ell$ as they induce a correlation between R_K and R_{K^*} that is opposite to the observed one.

Next, we perform fits to different sets of data within a frequentist approach in which the hadronic uncertainties are systematically included and minimized in the fits. We begin with the analysis of $R_{K^{(*)}}$ only, finding that the best fit is provided by combinations of the operators $\mathcal{O}_{9(10)}^\ell = \bar{s}\gamma^\mu b_L \ell\gamma_\mu(\gamma_5)\ell$ operators with a significance with respect to the Standard Model of $\sim 4\sigma$. An important conclusion of this analysis is that a lepton-specific contribution to \mathcal{O}_{10} is essential to understand the data. Under the hypothesis that new-physics couples selectively to the muons, we then present a series of fits to other $b \rightarrow s\mu\mu$ data with a conservative error assessment. First we include only the branching fraction of the $B_s \rightarrow \mu\mu$ decay, which provides a significant constraint that drifts the best fit point to a ‘‘chiral’’ left-handed solution $\mathcal{O}_9^\ell - \mathcal{O}_{10}^\ell$, but does not significantly increase the tension of the data with the SM.

In the last fit we include all the angular observables measured by LHCb, ATLAS, CMS and Belle for the bins below 6 GeV^2 . As previous fits in the literature, measurements of the angular observables tend to pull the Wilson coefficient δC_9^μ to negative values with a significance of more than 3σ , while rendering δC_{10}^μ consistent with 0 at $\sim 1\sigma$. The results of these fits, rephrased in terms of $C_{L/R}^\mu = (C_9^\mu \mp C_{10}^\mu)/2$, show that C_L^μ is very well determined by the fit $\delta C_L^\mu \simeq -1$ while C_R^μ is not. We have also noted, however, the potential vulnerability of the results of this fit to underlying assumptions regarding the hadronic uncertainties, as it

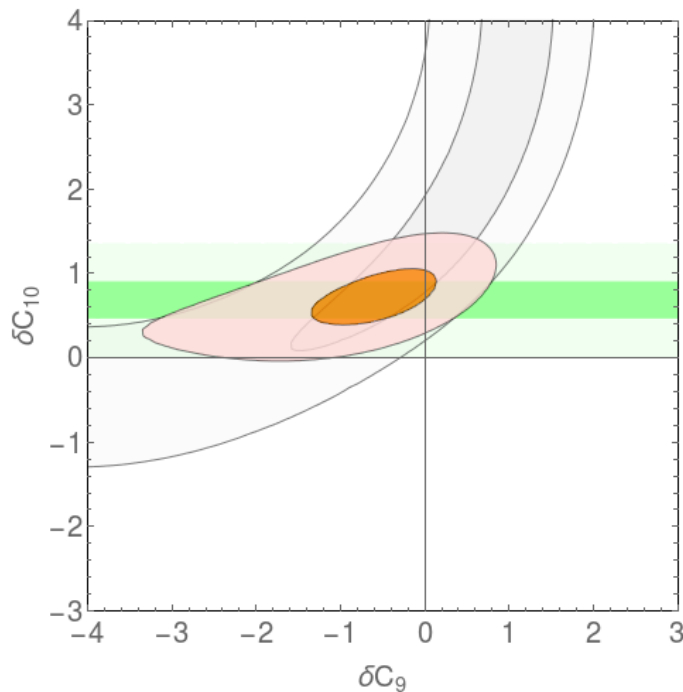


FIG. 9: Constraining power of the hypothetical measurement of R'_6 in the bin $[0.045, 1.1]$ GeV^2 discussed in the main text, represented at 1σ and 3σ by the horizontal green bands. This is shown overlaid to the 1σ and 3σ gray, arc-shaped regions given by the fit to the LUV observables R_K and R_{K^*} discussed in Sec. IV A and plotted in Fig. 3. The combination of the two constraints results in the regions plotted with orange and light-red colors.

has been discussed extensively in the literature. In order to quantify this, we have made a study of the robustness of the tensions of the SM with the data for different assumptions regarding the size of the hadronic uncertainties. We emphasize again that this problem is absent in the fits to only $R_{K^{(*)}}$ and $B_s \rightarrow \mu\mu$ and the respective statistical information inferred from the χ^2 is driven, in this case, by experimental uncertainties only so that its interpretation is free from theoretical ambiguities.

Therefore, we introduce and discuss a group of lepton-universality ratios all related to the coefficient of the angular distribution I_6 (or the forward-backward asymmetry) which are very sensitive to lepton nonuniversality in the Wilson coefficient C_{10}^ℓ and are largely insensitive to new-physics contributions to C_9 in the low- q^2 bin. A measurement of these observables would break the correlation between the lepton-specific effects in \mathcal{O}_9^ℓ and \mathcal{O}_{10}^ℓ observed in the fits to R_K and R_{K^*} . In light of the fact that the two observables P_2 have been measured by the LHCb for electrons and muons respectively at very low q^2 (though using a different binning), one is tempted to think that a measurement of the ratios proposed in this paper is feasible in the near future. We present prospects of the impact of such a measurement in the (C_9^ℓ, C_{10}^ℓ) plane, which could help clarifying the nature of the observed effects and contribute to the discovery of the new physics in $b \rightarrow s\ell\ell$ transitions.

VII. ACKNOWLEDGMENTS

We would like to thank Kostas Petridis and Luiz Vale Silva for helpful discussions. This work is partly supported by the National Natural Science Foundation of China under Grants No. 11375024 and No. 11522539 and by the US Department of Energy under grant DE-SC0009919. SJ is supported by an IPPP Associateship, STFC consolidated grant ST/L000504/1, and a Weizmann Institute “Weizmann-UK Making Connections” grant, and would like to thank STFC for past provision of HPC computing time.

-
- [1] G. Hiller and F. Kruger, Phys. Rev. **D69**, 074020 (2004), hep-ph/0310219.
 - [2] M. Bordone, G. Isidori, and A. Pattori, Eur. Phys. J. **C76**, 440 (2016), 1605.07633.
 - [3] J. T. Wei et al. (Belle), Phys. Rev. Lett. **103**, 171801 (2009), 0904.0770.
 - [4] J. P. Lees et al. (BaBar), Phys. Rev. **D86**, 032012 (2012), 1204.3933.

- [5] J. P. Lees et al. (BaBar), Phys. Rev. Lett. **112**, 211802 (2014), 1312.5364.
- [6] R. Aaij et al. (LHCb), Phys. Rev. Lett. **113**, 151601 (2014), 1406.6482.
- [7] S. Bifani, in *LHCb Seminar at CERN* (April 18th 2017), URL <https://indico.cern.ch/event/580620/>.
- [8] R. Aaij et al. (LHCb), Phys. Rev. Lett. **111**, 191801 (2013), 1308.1707.
- [9] R. Aaij et al. (LHCb), JHEP **02**, 104 (2016), 1512.04442.
- [10] S. Wehle et al. (Belle) (2016), 1612.05014.
- [11] T. A. collaboration (ATLAS) (2017).
- [12] M. Dinardo, in *52nd Rencontres de Moriond, La Thuile, March 18-25, 2017* (2017), URL <https://indico.in2p3.fr/event/13763/session/10/contribution/108/material/slides/0.pdf>.
- [13] R. Aaij et al. (LHCb), JHEP **06**, 133 (2014), 1403.8044.
- [14] R. Aaij et al. (LHCb), JHEP **06**, 115 (2015), 1503.07138.
- [15] R. Aaij et al. (LHCb), JHEP **09**, 179 (2015), 1506.08777.
- [16] F. Beaujean, C. Bobeth, and D. van Dyk, Eur. Phys. J. **C74**, 2897 (2014), [Erratum: Eur. Phys. J.C74,3179(2014)], 1310.2478.
- [17] S. Descotes-Genon, L. Hofer, J. Matias, and J. Virto, JHEP **06**, 092 (2016), 1510.04239.
- [18] W. Altmannshofer, C. Niehoff, P. Stangl, and D. M. Straub (2017), 1703.09189.
- [19] M. Beneke, T. Feldmann, and D. Seidel, Nucl. Phys. **B612**, 25 (2001), hep-ph/0106067.
- [20] B. Grinstein and D. Pirjol, Phys. Rev. **D70**, 114005 (2004), hep-ph/0404250.
- [21] U. Egede, T. Hurth, J. Matias, M. Ramon, and W. Reece, JHEP **11**, 032 (2008), 0807.2589.
- [22] A. Khodjamirian, T. Mannel, A. A. Pivovarov, and Y. M. Wang, JHEP **09**, 089 (2010), 1006.4945.
- [23] M. Beylich, G. Buchalla, and T. Feldmann, Eur. Phys. J. **C71**, 1635 (2011), 1101.5118.
- [24] A. Khodjamirian, T. Mannel, and Y. M. Wang, JHEP **02**, 010 (2013), 1211.0234.
- [25] S. Jäger and J. Martin Camalich, JHEP **05**, 043 (2013), 1212.2263.
- [26] R. R. Horgan, Z. Liu, S. Meinel, and M. Wingate, Phys. Rev. Lett. **112**, 212003 (2014), 1310.3887.
- [27] J. Lyon and R. Zwicky (2014), 1406.0566.
- [28] S. Descotes-Genon, L. Hofer, J. Matias, and J. Virto, JHEP **12**, 125 (2014), 1407.8526.
- [29] S. Jäger and J. Martin Camalich, Phys. Rev. **D93**, 014028 (2016), 1412.3183.
- [30] A. Bharucha, D. M. Straub, and R. Zwicky, JHEP **08**, 098 (2016), 1503.05534.
- [31] M. Ciuchini, M. Fedele, E. Franco, S. Mishima, A. Paul, L. Silvestrini, and M. Valli, JHEP **06**, 116 (2016), 1512.07157.
- [32] S. Bra, G. Hiller, and I. Nisandzic, Eur. Phys. J. **C77**, 16 (2017), 1606.00775.
- [33] R. Aaij et al. (LHCb), Eur. Phys. J. **C77**, 161 (2017), 1612.06764.
- [34] T. Hurth, F. Mahmoudi, and S. Neshatpour, Nucl. Phys. **B909**, 737 (2016), 1603.00865.
- [35] B. Capdevila, S. Descotes-Genon, L. Hofer, and J. Matias (2017), 1701.08672.
- [36] V. G. Chobanova, T. Hurth, F. Mahmoudi, D. Martinez Santos, and S. Neshatpour (2017), 1702.02234.
- [37] R. Alonso, B. Grinstein, and J. Martin Camalich, Phys. Rev. Lett. **113**, 241802 (2014), 1407.7044.
- [38] G. Hiller and M. Schmaltz, Phys. Rev. **D90**, 054014 (2014), 1408.1627.
- [39] D. Ghosh, M. Nardecchia, and S. A. Renner, JHEP **12**, 131 (2014), 1408.4097.
- [40] T. Hurth, F. Mahmoudi, and S. Neshatpour, JHEP **12**, 053 (2014), 1410.4545.
- [41] W. Altmannshofer and D. M. Straub, Eur. Phys. J. **C75**, 382 (2015), 1411.3161.
- [42] B. Capdevila, S. Descotes-Genon, J. Matias, and J. Virto, JHEP **10**, 075 (2016), 1605.03156.
- [43] N. Serra, R. Silva Coutinho, and D. van Dyk, Phys. Rev. **D95**, 035029 (2017), 1610.08761.
- [44] B. Grinstein, M. J. Savage, and M. B. Wise, Nucl. Phys. **B319**, 271 (1989).
- [45] G. Buchalla, A. J. Buras, and M. E. Lautenbacher, Rev. Mod. Phys. **68**, 1125 (1996), hep-ph/9512380.
- [46] K. G. Chetyrkin, M. Misiak, and M. Munz, Phys. Lett. **B400**, 206 (1997), [Erratum: Phys. Lett.B425,414(1998)], hep-ph/9612313.
- [47] C. Bobeth, G. Hiller, and G. Piranishvili, JHEP **12**, 040 (2007), 0709.4174.
- [48] R. Aaij et al. (LHCb), JHEP **04**, 064 (2015), 1501.03038.
- [49] A. Paul and D. M. Straub, JHEP **04**, 027 (2017), 1608.02556.
- [50] M. Beneke and T. Feldmann, Nucl. Phys. **B592**, 3 (2001), hep-ph/0008255.
- [51] A. Hocker, H. Lacker, S. Laplace, and F. Le Diberder, Eur. Phys. J. **C21**, 225 (2001), hep-ph/0104062.
- [52] K. De Bruyn, R. Fleischer, R. Kneegjens, P. Koppenburg, M. Merk, A. Pellegrino, and N. Tuning, Phys. Rev. Lett. **109**, 041801 (2012), 1204.1737.
- [53] C. Bobeth, M. Gorbahn, T. Hermann, M. Misiak, E. Stamou, and M. Steinhauser, Phys. Rev. Lett. **112**, 101801 (2014), 1311.0903.
- [54] S. Aoki et al., Eur. Phys. J. **C77**, 112 (2017), 1607.00299.
- [55] W. Altmannshofer, C. Niehoff, and D. M. Straub (2017), 1702.05498.
- [56] T. E. Coan et al. (CLEO), Phys. Rev. Lett. **84**, 5283 (2000), hep-ex/9912057.
- [57] M. Nakao et al. (Belle), Phys. Rev. **D69**, 112001 (2004), hep-ex/0402042.
- [58] B. Aubert et al. (BaBar), Phys. Rev. Lett. **103**, 211802 (2009), 0906.2177.
- [59] C. Patrignani et al. (Particle Data Group), Chin. Phys. **C40**, 100001 (2016).
- [60] T. Horiguchi et al. (Belle) (2017), 1707.00394.
- [61] R. Aaij et al. (LHCb), JHEP **05**, 159 (2013), 1304.3035.
- [62] S. Jger, K. Leslie, M. Kirk, and A. Lenz (2017), 1701.09183.
- [63] S. Descotes-Genon, T. Hurth, J. Matias, and J. Virto, JHEP **05**, 137 (2013), 1303.5794.